results from the far more extensive dye tracing programs of 1990 and 1991 [*Nienow et al.*, 1998] to indicate that at Haut Glacier d'Arolla the spatial pattern of subglacial channel evolution would be similar for each year. In addition, results from water level/pressure measurements within extensive borehole arrays over several years (1992–1995) suggest that subglacial drainage axes tend to form in approximately the same location each year [*Gordon*, 1996]. It is therefore likely that channelized drainage evolved along the eastern VPA/PDA. The center of the measured VPA lies close to the predicted PDA (Figures 6b–6g). Moulins, which mark the points of entry of surface streams into the glacier, tend to be clustered along the line of the major subglacial drainage pathways (Figures 6b–6g). The inferred status of channel development is shown for each time period in Figures 6b–6g, based upon analysis of Figure 2. From the above interpretation of the dye tracing experiments it seems evident that the majority of moulins in at least the lower 3 km of the glacier became connected to an efficient channelized drainage system during the course of the 1995 melt season. However, dye injections at moulin B (located 1.75 km up glacier, Figure 1) suggest that it remained hydraulically isolated from the channelized drainage system. Tests undertaken on 23 July (J.D. 204) and 7 August (J.D. 219) resulted in through flow velocities of ~0.14 m s^{-1}, while tests from sites farther up glacier were generating through flow velocities of between 0.31 and 0.57 m s^{-1} (Figure 2). The results from moulin B are consistent with those from tracing work in 1990 and 1991 which indicate that within the lower glacier some moulins are connected to a residual section of inefficient distributed drainage that persisted in interchannel areas throughout the melt season (P. Nienow et al., The spatial extent of channelised and distributed subglacial drainage systems: Implications for ice dynamics and subglacial sediment evacuation, submitted to *Hydrolical Processes*, 2001).

5. EOF Analysis of Surface Velocity Fields

[13] Spatial patterns of surface longitudinal velocity for periods throughout the 1995 melt season were analyzed in terms of empirical orthogonal functions (EOFs). A schematic cartoon, illustrating the basic concepts of the analysis, is included to help explain the following summary (Figure 8). The method is reviewed and explained in full by *Peixoto and Oort* [1992, pp. 67–69, Appendix B, p. 492]. Since its introduction in the atmospheric sciences in the 1950s, this type of analysis has also been widely used in hydrology, oceanography, and solid earth geophysics. It has not been used previously to study temporal and spatial patterns of glacier motion. The measured surface velocities from 31 stakes over 31 days between 25 June and 6 August (J.D. 176 and J.D. 218) are organized into a matrix where each row represents a single stake and each column represents a single day (gaps in the velocity records of some stakes are filled with spatially interpolated values). The square of this matrix is then decomposed into 31 normalized eigenvectors and 31 eigenvalues. When the elements of the individual eigenvectors are mapped to the 31 stake locations on the glacier, they define distinct spatial modes (or EOFs) of surface velocity (Figure 9). The observed spatial velocity pattern, at any given time, can be exactly reconstructed by weighting each of the linearly independent EOFs (by multiplying it by its coefficient) and adding them together. The time series of the coefficients of each mode (Figure 10) indicate the relative strength and sign (positive or negative) of each mode at any given time. The eigenvalues associated with each EOF, divided by the sum of all the eigenvalues, indicate the proportion of the total variance in velocity patterns, throughout the melt season, accounted for by each EOF. The EOF modes are arranged in decreasing order according to the percentage of variance explained by them. Thus the EOF analysis breaks down the data into a set of linearly independent modes, each of which accounts for a certain percentage of the total spatial and temporal variance within the original data.

[14] Unlike most other orthogonal representations, the EOFs are derived directly from the data themselves rather than being a predetermined orthogonal set of analytical functions (e.g., Fourier analysis). Furthermore, the first few EOF modes usually explain a much higher fraction of the total variance than the same number of other orthogonal functions. Thus fewer empirical functions are usually required to explain the same amount of variance in the data. EOF analysis and principal components analysis (PCA) [*Johnston*, 1980] both solve for the eigenvectors and eigenvalues of the same correlation matrix. Although the terms "principal component" and "EOF" describe the same orthogonal functions, the results are used differently. PCA involves correlating the individual time series at each original grid point with the coefficient time series of each principal component (or EOF). The results are then clustered according to which principal component correlates best with each grid point. Some points will correlate best with principal component 1, and others will correlate best with principal component 2, etc. In PCA, the spatial plots of the various principal components (or EOFs) are not analyzed. In the EOF analysis presented here, we look at the spatial patterns of the different EOF modes to determine whether the patterns of the most dominant modes can be interpreted physically. The EOF modes which account for a large fraction of the variance are, in general, considered to be physically meaningful, while the higher-order EOF modes represent minor features and smaller-scale fluctuations and are most likely due to sampling and measurement errors.

[15] Without de-trending the original data, a contour plot of the most dominant EOF mode shows a regular parabolic pattern (Figure 9a). This pattern is virtually identical to the long-term mean surface velocity pattern (Figure 6a) and is indicative of the background low-frequency variability due to ice deformation and long-term, average basal motion. In the results presented here, the input data have been temporally de-trended before analysis. This effectively removes the background, long-term pattern due to ice deformation and average basal motion, which otherwise accounts for over 90% of all spatial variation in surface velocity throughout the melt season. De-trending the data makes it easier to identify spatial patterns of surface velocity which are statistically significant but act over shorter timescales. EOFs 1 and 2 (Figures 9b and 9c) account for 74.33% and 14.62%,

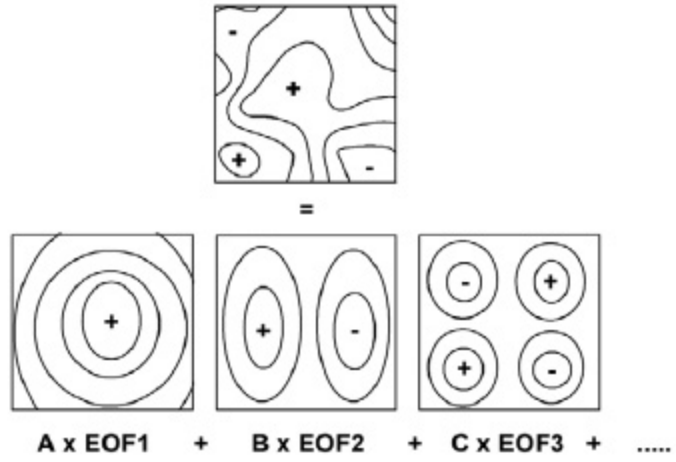

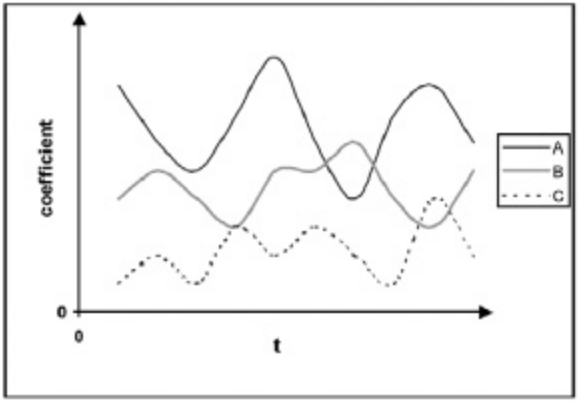

Figure 8. Schematic cartoon illustrating the essential elements of the empirical orthogonal function (EOF) analysis.